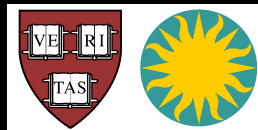


Overview of CMB Foreground Simulations

Angelica de Oliveira-Costa



Harvard-Smithsonian
Center for Astrophysics

CMB Foreground Simulations

One of the main challenges facing microwave experiments is to distinguish the cosmological signal from the foreground contamination.

Definition: what is a Foreground and what is a Signal? Where should we draw the line?

Historically, the CMB community agrees that effects occurring around or before recombination ($z \sim 10^3$) constitute a signal, whereas **dust, free-free and synchrotron radiation** (regardless if they are Galactic in origin or not) are foregrounds.

When taking a more goal-oriented approach, where the goal is to measure cosmological parameters, the issue is not when or how the signal was calculated, but how reliably it can be calculated. Therefore, a more operational definition of foreground was created:

A foreground is an effect whose dependence on cosmological parameters we cannot compute accurately from first principles at the present time.

Objectives: why people study foregrounds? Why people do foreground simulations?

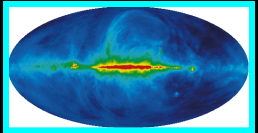
1) Simulations are a vital: accurate modeling and subtraction of the foreground contamination is necessary in order to correct the measured CMB power spectrum. To do a good job on removing foregrounds, we need to understand their frequency and scale dependence, frequency coherence, and better characterize their non-Gaussian behavior. In addition, foreground simulations also help to optimize scan strategy and data analysis pipelines.

2) Unique opportunity to understand non-cosmological processes on the microwave frequencies.

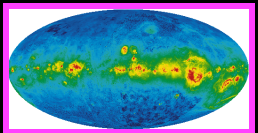
CMB Foreground Simulations

What are the Emission Mechanisms associated to the foregrounds?

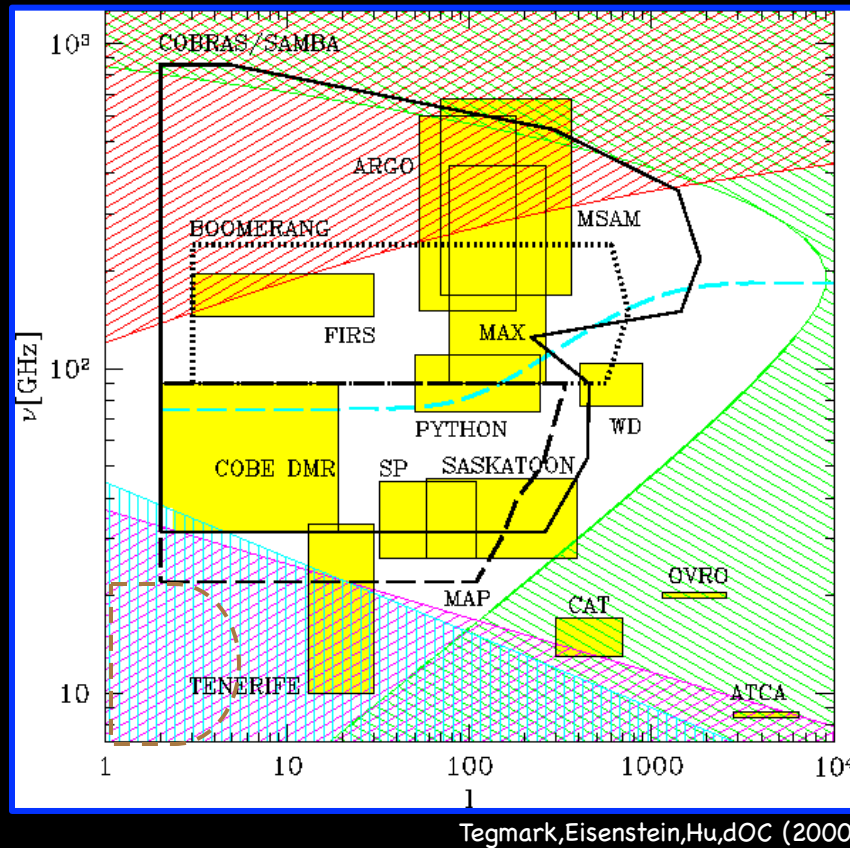
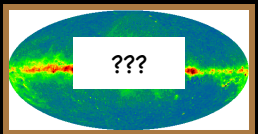
Synchrotron, 408 MHz



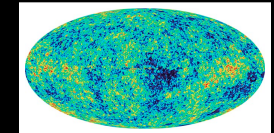
Free-free, 460 THz



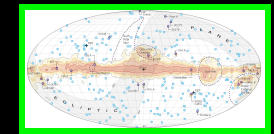
Foreground-X



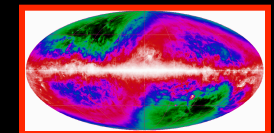
CMB



Point Sources



Dust, 3000 GHz



Foregrounds discussed on this review:

Non-cosmological processes between 1-100 GHz. Galactic foregrounds (dust, free-free and synchrotron radiation) and extra galactic point sources.

Notation:

We defined C_l in the usual manner, as the variance of the amplitude of the fluctuations in the l -th multipole. We then model the power spectra of all components as power laws, $C_l = A \nu^\alpha / l^\beta$

CMB Foreground Simulations

Synchrotron Emission:

This foreground is model as power law: $C_l = A \nu^\alpha / \beta$

The spectral index α depends on the energy distribution of the relativistic electrons, therefore it varies across the sky. It is also expected a spectral steepening towards higher frequencies, corresponding to a softer electron spectrum (Banday & Wolfendale, 1981).

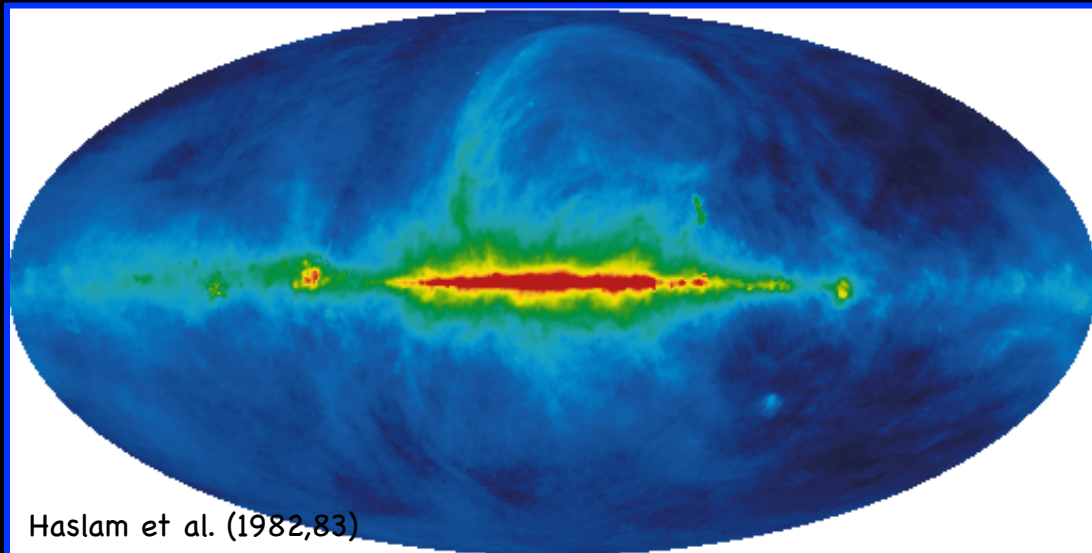
Unpolarized Synchrotron Emission (slopes α and β):

Haslam ($\theta \sim 1^\circ$): $\alpha = -2.8 \pm 0.15$ (Platania et al. 98) & $-3.0 < \beta < -2.5$ (TE96, Bouchet et al. 96).

Reich & Reich ($\theta \sim 35'$) + **Haslam**: $-3.2 < \alpha < -2.9$ and $-3.0 < \beta < -2.6$ (La Porta et al. 10).

Rhodes ($\theta = 20'$): $\alpha \sim -2.8$ with strong variation across the sky & $\beta = -2.92 \pm 0.07$ (Giardino et al. 01).

There is a good agreement between the **WMAP K-band** & the extrapolated **Haslam 408 MHz** map (Page et al. 2007).



The synchrotron emission is modeled as an extrapolation in frequency of the **Haslam 408 MHz** map, ie, the synchrotron emission map T_ν , at frequency ν , is given by:

$$T_\nu = T_{408} (\nu/408)^\alpha$$

see, eg, PSM and Gold et al. (2010).

CMB Foreground Simulations

Planck Sky Model (PSM):

This Package provides IDL codes to generate full-sky predictions or constrained realizations of the CMB + foreground emissions in the range from 1 to 1000 GHz (Jacques Delabrouille). The PSM can be downloaded from:

<http://www.apc.univ-paris7.fr/~delabrou/PSM/psm.html>

There is also the Planck Simulator at <http://gavo.mpa-garching.mpg.de/planck/> that provides maps of the CMB + foregrounds at the Planck & WMAP frequencies (from 23 to 857 GHz).

CMB Foreground Simulations

Free-free Emission:

This foreground is model as power law: $C_l = A \nu^\alpha / l^\beta$

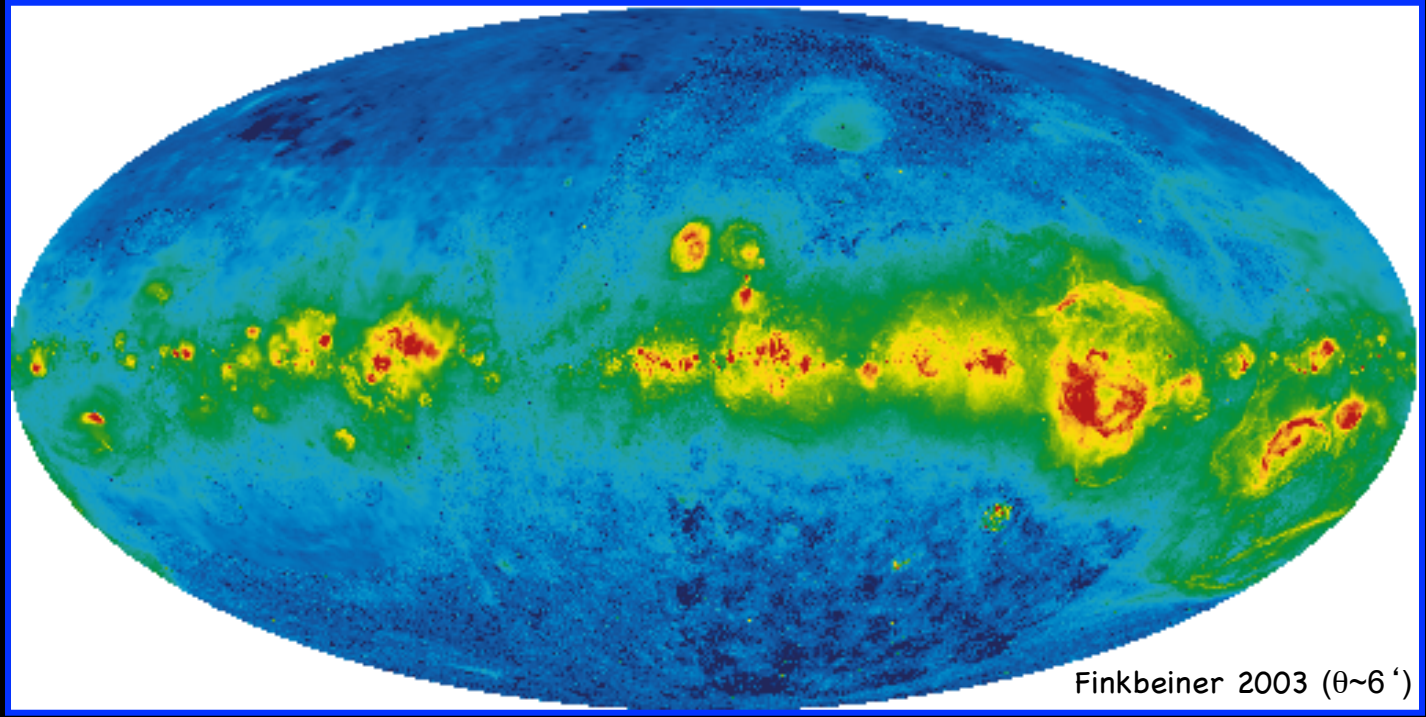
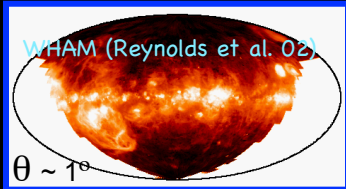
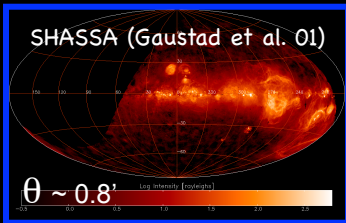
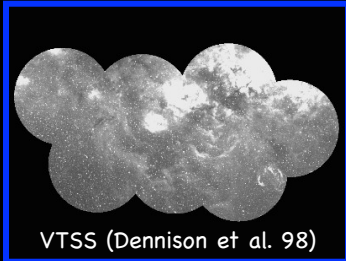
Of all the diffuse Galactic foregrounds, free-free is the one with best known frequency dependence ($\nu \sim -2.15$). H_α in emission, which is produced by the same Warm Ionized Medium (WIM) responsible for the Bremsstrahlung, is a tracer of Galactic free-free.

Unpolarized Synchrotron Emission (slopes α and β):

Although the spectrum of free-free emission is well known, the amplitude and power spectrum are not. From the WHAM survey at the Tenerife observing region (at $20^\circ < |b| < 30^\circ$): $\beta \sim -3.0$ for $10 < l < 40$ (de Oliveira-Costa et al. 2000).

CMB Foreground Simulations

Free-free Simulation:



Dickinson et al. (2003) derive an all-sky degree-scale free-free emission template from H_α surveys (SHASSA + WHAM). This map is then corrected for dust absorption using the 100 μm dust map of SDF. The final H_α map is used as a template for free-free emission - except in the region close to the Galactic plane ($|b| < 5^\circ$), where the effect of extinction is too high. The relationship between radio and H_α emission can be calculated as $T_{\text{ff}} \sim a(\nu, T_e) \nu^{-2.15} T_e^{0.667} I_{H\alpha}$, where frequency scaling is done between 1 to 1000 GHz with $T_e = 7000\text{K}$.

Similar analysis was performed by Dobler & Finkbeiner (2007).

Miville-Deschenes et al. (2008) produces a composite free-free map using the map from Dickinson et al. (2003) and the WMAP free-free MEM map (Gold et al. 2005). This composite map is used in the PSM.

CMB Foreground Simulations

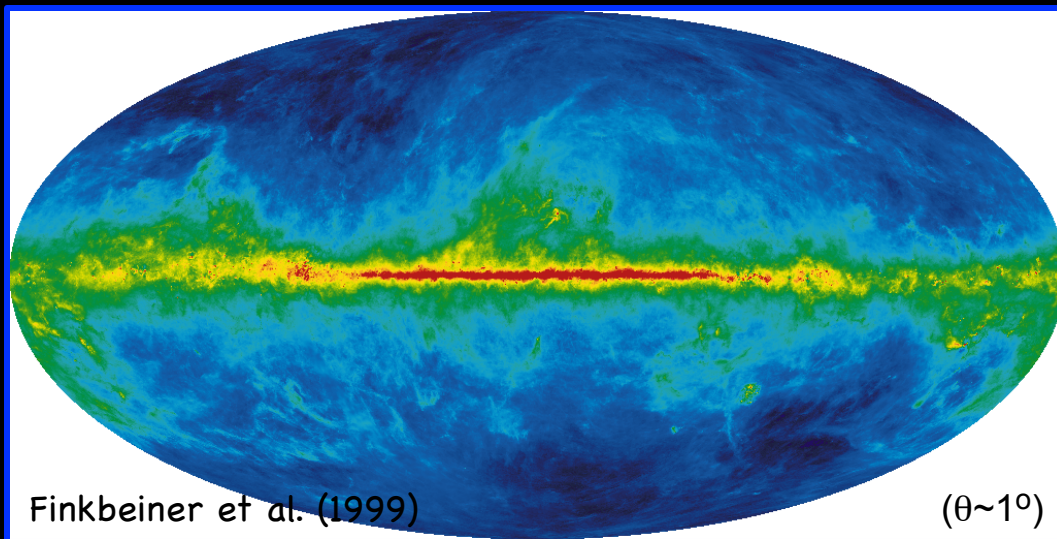
Dust Emission:

This foreground is model as power law: $C_l = A \nu^\alpha [e^{h\nu/kT} / (e^{h\nu/kT} - 1)] l^{-\beta}$

Unpolarized Dust Emission (slopes α and β):

From a combined analysis of **DIRBE & IRAS** data, it was observed that the Galactic dust emission can be model by a two temperature component model, with $T_{(1,2)} = 9.5$ K and 16 K and an emissivity of $\alpha_{(1,2)} = 1.7$ and 2.7 (Schlegel et al. 1998). Previous estimates of α have ranged between 1.4 - 2.0 (Reach et al. 1995; Kogut et al. 1996). From **BOOMERanG** 245 and 345 GHz channels, it was observed that the temperature of the dust component varies between 7-20 K, while the emissivity α varies between 1-5 (Veneziani et al. 2010).

Analysis of the **DIRBE** maps showed no evidence for a departure from $\beta = -3$ for $l < 300$ (Wright 1998). A combined **DIRBE & IRAS** analysis suggested $\beta = -2.5$ (Schlegel et al. 1998), while earlier works suggested $\beta \sim -3$ (Gautier et al. 1992, Low & Cutri 1994, Guarani et al. 1995, TE 1996). The **Archeops** experiment also suggested $\beta \sim -3$, after a cosecant was subtracted (Ponthieu et al. 2005).



The SFD map (Finkbeiner et al. 1999) and/or the IRAS 100 μm map can be used to model the dust emission, see, eg, the PSM.

CMB Foreground Simulations

Foreground X:

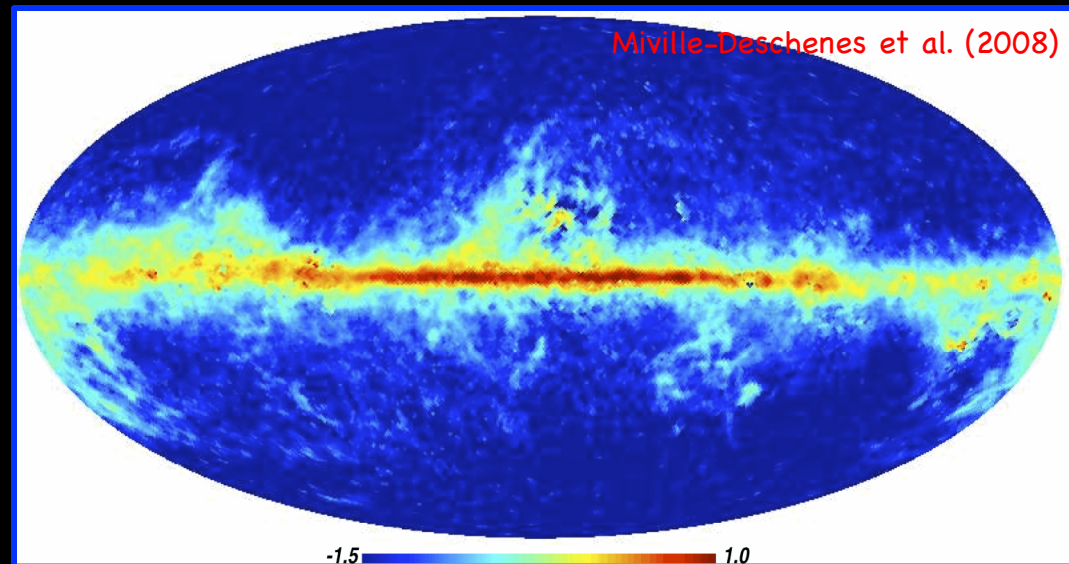
There is observational evidence in favor of a 4th component of emission in our Galaxy. This component, nicknamed Foreground-X, is spatially correlated with the 100 μm dust emission but with a spectrum that rising towards lower frequencies, subsequently flattening and turning down somewhere around 15 GHz. There are statistical (eg, **DMR, Saskatoon, OVRO, 19 GHz, Tenerife, SP94, WMAP, WMAP7+ARCADE2, etc.**), as well as, direct (eg, Finkbeiner et al. 2004) detections of this anomalous component.

Caveat: There is no template for this component.

Miville-Deschenes et al. (2008) produces a spinning dust template by removing the synchrotron and free-free emissions of the WMAP 23 GHz map - this residual map is shown to be well correlated with the SFD E(B-V) map. The scaling in frequency is done using a constant spectrum on the sky given by the Draine & Lazarian (1998) model for the WNM. This model is incorporated in the PSM.

Similar analysis was performed by Dobler & Finkbeiner (2007).

SpDust by Haimoud et al. (2009) is an IDL program that evaluates the spinning dust emissivity - publicly available from <http://www.tapir.caltech.edu/~yacine/spdust/spdust.html>



CMB Foreground Simulations

Modeling the diffuse emission from 10 MHz to 100 GHz

Ref	ν [GHz]	FWHM [$^{\circ}$]	Region		Observatory	Status
			RA	DEC		
(Alexander & Novaco 1974)	0.00393	60	$00^{\text{h}} < \alpha < 24^{\text{h}}$	$-60^{\circ} < \delta < +60^{\circ}$	RAE-1	D
(Alexander & Novaco 1974)	0.00655	60	$00^{\text{h}} < \alpha < 24^{\text{h}}$	$-60^{\circ} < \delta < +60^{\circ}$	RAE-1	D
(Caswell 1976)	0.010	2.6x1.9	$00^{\text{h}} < \alpha < 16^{\text{h}}$	$-06^{\circ} < \delta < +74^{\circ}$	DRAO, CAN	A
(Cane & Erickson 2001)	0.010	5	$00^{\text{h}} < \alpha < 24^{\text{h}}$	$-65^{\circ} < \delta < +90^{\circ}$	DRAO(CAN),AUS	D
(Hamilton & Haynes 1968)	0.0102	4x5	$00^{\text{h}} < \alpha < 24^{\text{h}}$	$-65^{\circ} < \delta < -02^{\circ}$	AUS	D
(Bridle 1967)	0.0135	53x12	$00^{\text{h}} < \alpha < 24^{\text{h}}$	$(16,35,52,69)^{\circ}$	ENG	C
(Ellis 1982)	0.0165	1.5	$00^{\text{h}} < \alpha < 24^{\text{h}}$	$-90^{\circ} < \delta < 00^{\circ}$	Tasmania, AUS	D
(Bridle 1967)	0.0175	12x17	$00^{\text{h}} < \alpha < 24^{\text{h}}$	$(16,35,52,69)^{\circ}$	ENG	C
(Roger et al. 1999)	0.022	1.1x1.7	$00^{\text{h}} < \alpha < 24^{\text{h}}$	$-28^{\circ} < \delta < +80^{\circ}$	DRAO, CAN	A
(Turtle et al. 1962)	0.026	15x44	$00^{\text{h}} < \alpha < 24^{\text{h}}$	$(20,40,60)^{\circ}$	ENG	C
(Mathewson et al. 1965)	0.030	11	$00^{\text{h}} < \alpha < 24^{\text{h}}$	$-90^{\circ} < \delta < 00^{\circ}$	Parkes, AUS	D
(Cane 1978)	0.030	11	$00^{\text{h}} < \alpha < 24^{\text{h}}$	$-90^{\circ} < \delta < +90^{\circ}$		D
(Dwarakanath & Shankar 1990)	0.0345	0.4x0.7	$00^{\text{h}} < \alpha < 24^{\text{h}}$	$-30^{\circ} < \delta < +60^{\circ}$	GEETEE, IND	A
(Milogradov-Turin & Smith 1973)	0.038	7.5	$00^{\text{h}} < \alpha < 24^{\text{h}}$	$-25^{\circ} < \delta < +70^{\circ}$	Jodrell Bank, ENG	D
(Turtle et al. 1962)	0.038	15x44	$00^{\text{h}} < \alpha < 24^{\text{h}}$	$(20,40,60)^{\circ}$	ENG	C
(Alvarez 1997)	0.045	4.6x2.4	$00^{\text{h}} < \alpha < 24^{\text{h}}$	$-90^{\circ} < \delta < +19^{\circ}$	CHL	B
(Maeda et al. 1999)	0.045	3.6x3.6	$00^{\text{h}} < \alpha < 24^{\text{h}}$	$+05^{\circ} < \delta < +65^{\circ}$	JPN	B
(Bridle 1967)	0.0815	12x17	$00^{\text{h}} < \alpha < 24^{\text{h}}$	$(16,25,30,35,40,52,69)^{\circ}$	ENG	C
(Landecker & Wielebinski 1970)	0.085	3.8x3.5	$00^{\text{h}} < \alpha < 24^{\text{h}}$	$-25^{\circ} < \delta < +25^{\circ}$	Parkes, AUS	C,A
(Bolton & Westfold 1950)	0.100	17	$00^{\text{h}} < \alpha < 24^{\text{h}}$	$-90^{\circ} < \delta < +30^{\circ}$	AUS	D
(Landecker & Wielebinski 1970)	0.150	2.2x2.2	$00^{\text{h}} < \alpha < 24^{\text{h}}$	$-25^{\circ} < \delta < +25^{\circ}$	Parkes, AUS	C,A
(Hamilton & Haynes 1969)	0.153	2.2	$00^{\text{h}} < \alpha < 24^{\text{h}}$	$-90^{\circ} < \delta < +05^{\circ}$	Parkes, AUS	D
(Reber 1944)	0.160	8x6	$16^{\text{h}} < \alpha < 22^{\text{h}}$	$-33^{\circ} < \delta < +90^{\circ}$	Wheaton, USA	D
(Turtle et al. 1962)	0.176	15x44	$00^{\text{h}} < \alpha < 24^{\text{h}}$	$(20,40,60)^{\circ}$	ENG	C
(Turtle & Baldwin 1962)	0.178	0.2x4.6	$00^{\text{h}} < \alpha < 24^{\text{h}}$	$-05^{\circ} < \delta < +90^{\circ}$	ENG	D
(Allen & Gum 1950)	0.200		$00^{\text{h}} < \alpha < 24^{\text{h}}$	$-90^{\circ} < \delta < +45^{\circ}$	Commonwealth, AUS	D
(Dröge & Priester 1956)	0.200	16.8	$00^{\text{h}} < \alpha < 24^{\text{h}}$	$-20^{\circ} < \delta < +90^{\circ}$	Kieler, GER	D
(Turtle et al. 1962)	0.400	8.5x6.5	$00^{\text{h}} < \alpha < 24^{\text{h}}$	$(20,40,60)^{\circ}$	ENG	C
(Pauliny-Toth & Shakeshaft 1962)	0.404	7.5	$00^{\text{h}} < \alpha < 24^{\text{h}}$	$-20^{\circ} < \delta < +90^{\circ}$	ENG	C
(Haslam et al. 1982)	0.408	0.8	$00^{\text{h}} < \alpha < 24^{\text{h}}$	$-90^{\circ} < \delta < +90^{\circ}$	GER, AUS, ENG	A
(Berkhuijsen 1972)	0.820	1.2	$00^{\text{h}} < \alpha < 24^{\text{h}}$	$-07^{\circ} < \delta < +85^{\circ}$	Dwingeloo, NLD	C,A
(Reich 1982; Reich & Reich 1986)	1.42	0.6	$00^{\text{h}} < \alpha < 24^{\text{h}}$	$-19^{\circ} < \delta < +90^{\circ}$	Stockert, GER	A
(Reich et al. 2001)	1.42	0.6	$00^{\text{h}} < \alpha < 24^{\text{h}}$	$-90^{\circ} < \delta < -10^{\circ}$	Villa Elisa, ARG	B
(Tello et al. 2007)	2.3	2.3x1.9	$00^{\text{h}} < \alpha < 24^{\text{h}}$	$-53^{\circ} < \delta < +35^{\circ}$	BRA	D
(Jonas et al. 1998)	2.326	0.3	$00^{\text{h}} < \alpha < 24^{\text{h}}$	$-83^{\circ} < \delta < +32^{\circ}$	Hartebeesthoek, ZAF	B
(Cottingham 1987; Boughn et al. 1992)	19	3	$00^{\text{h}} < \alpha < 24^{\text{h}}$	$-15^{\circ} < \delta < +75^{\circ}$	Ballou, USA	B
(This Work)	23	0.88	$00^{\text{h}} < \alpha < 24^{\text{h}}$	$-90^{\circ} < \delta < +90^{\circ}$	WMAP	A
(Bennett et al. 1996)	31	7	$00^{\text{h}} < \alpha < 24^{\text{h}}$	$-90^{\circ} < \delta < +90^{\circ}$	COBE/DMR	A
(This Work)	33	0.66	$00^{\text{h}} < \alpha < 24^{\text{h}}$	$-90^{\circ} < \delta < +90^{\circ}$	WMAP	A
(This Work)	41	0.51	$00^{\text{h}} < \alpha < 24^{\text{h}}$	$-90^{\circ} < \delta < +90^{\circ}$	WMAP	A
(Bennett et al. 1996)	53	7	$00^{\text{h}} < \alpha < 24^{\text{h}}$	$-90^{\circ} < \delta < +90^{\circ}$	COBE/DMR	A
(This Work)	61	0.35	$00^{\text{h}} < \alpha < 24^{\text{h}}$	$-90^{\circ} < \delta < +90^{\circ}$	WMAP	A
(Bennett et al. 1996)	90	7	$00^{\text{h}} < \alpha < 24^{\text{h}}$	$-90^{\circ} < \delta < +90^{\circ}$	COBE/DMR	A
(This Work)	94	0.22	$00^{\text{h}} < \alpha < 24^{\text{h}}$	$-90^{\circ} < \delta < +90^{\circ}$	WMAP	A

A = Publicly available in digital form.

B = Available on request.

C = Available as printed table (which we OCRred).

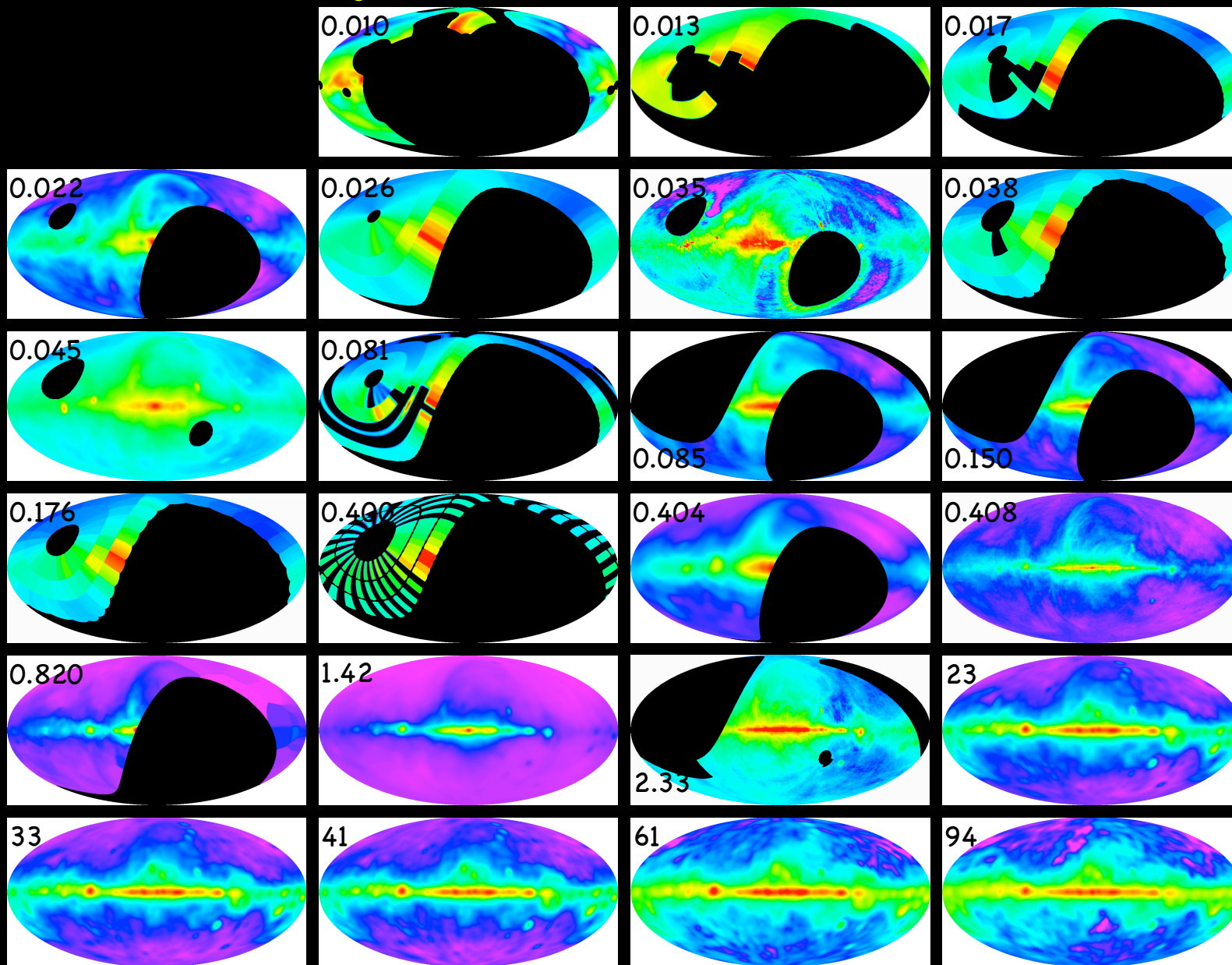
D = Not available in any numerical form.

dOC, Tegmark, Gaensler, Jonas, Landecker, Reich (2008)

<https://www.cfa.harvard.edu/~adeolive/gsm/> or <http://lambda.gsfc.nasa.gov/toolbox/>

CMB Foreground Simulations

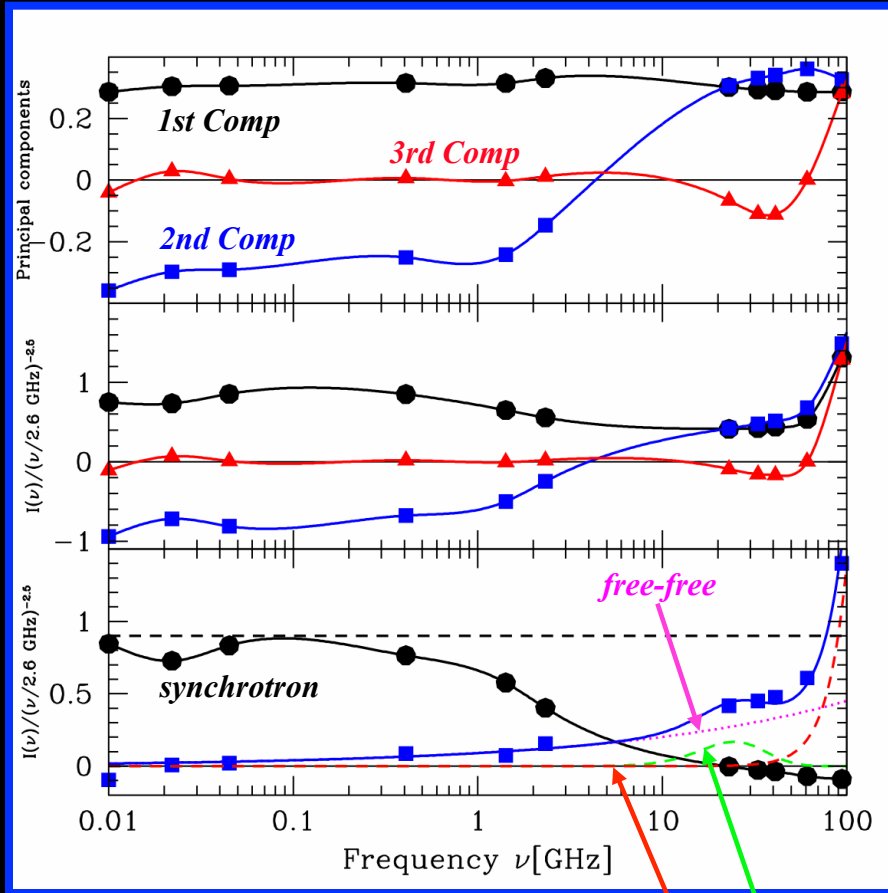
Modeling the diffuse emission from 10 MHz to 100 GHz



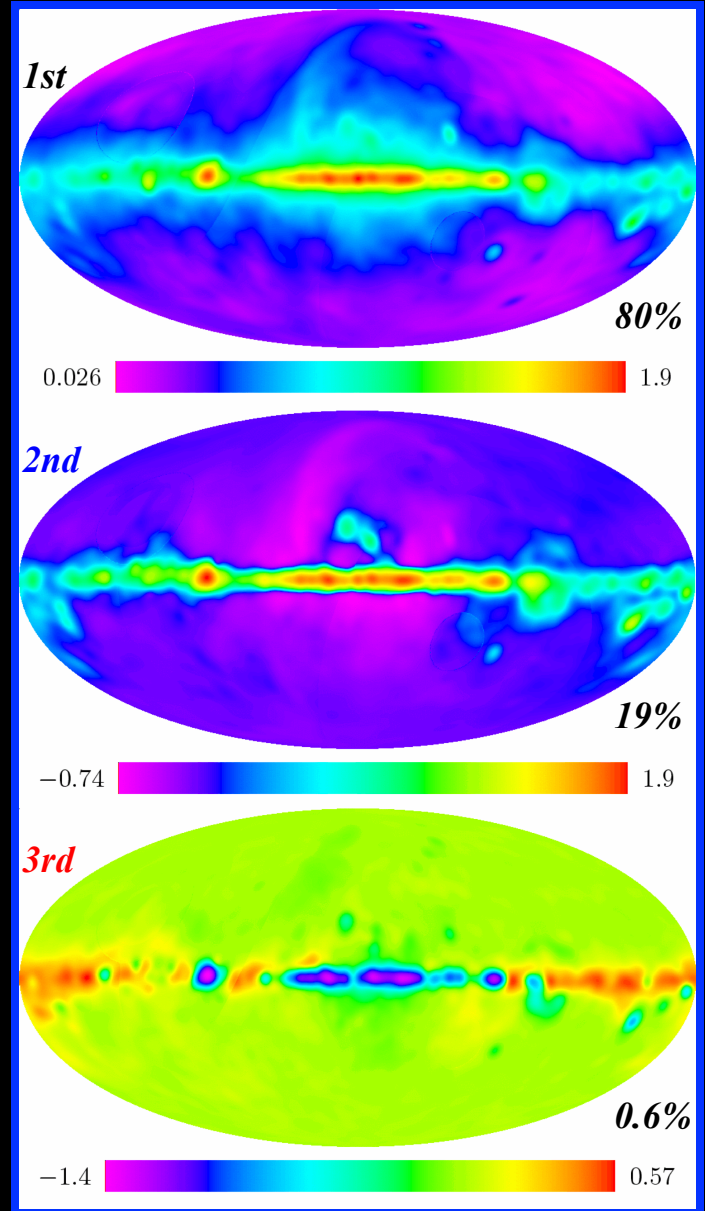
CMB Foreground Simulations

Modeling the diffuse emission from 10 MHz to 100 GHz

Principal Component Analysis:

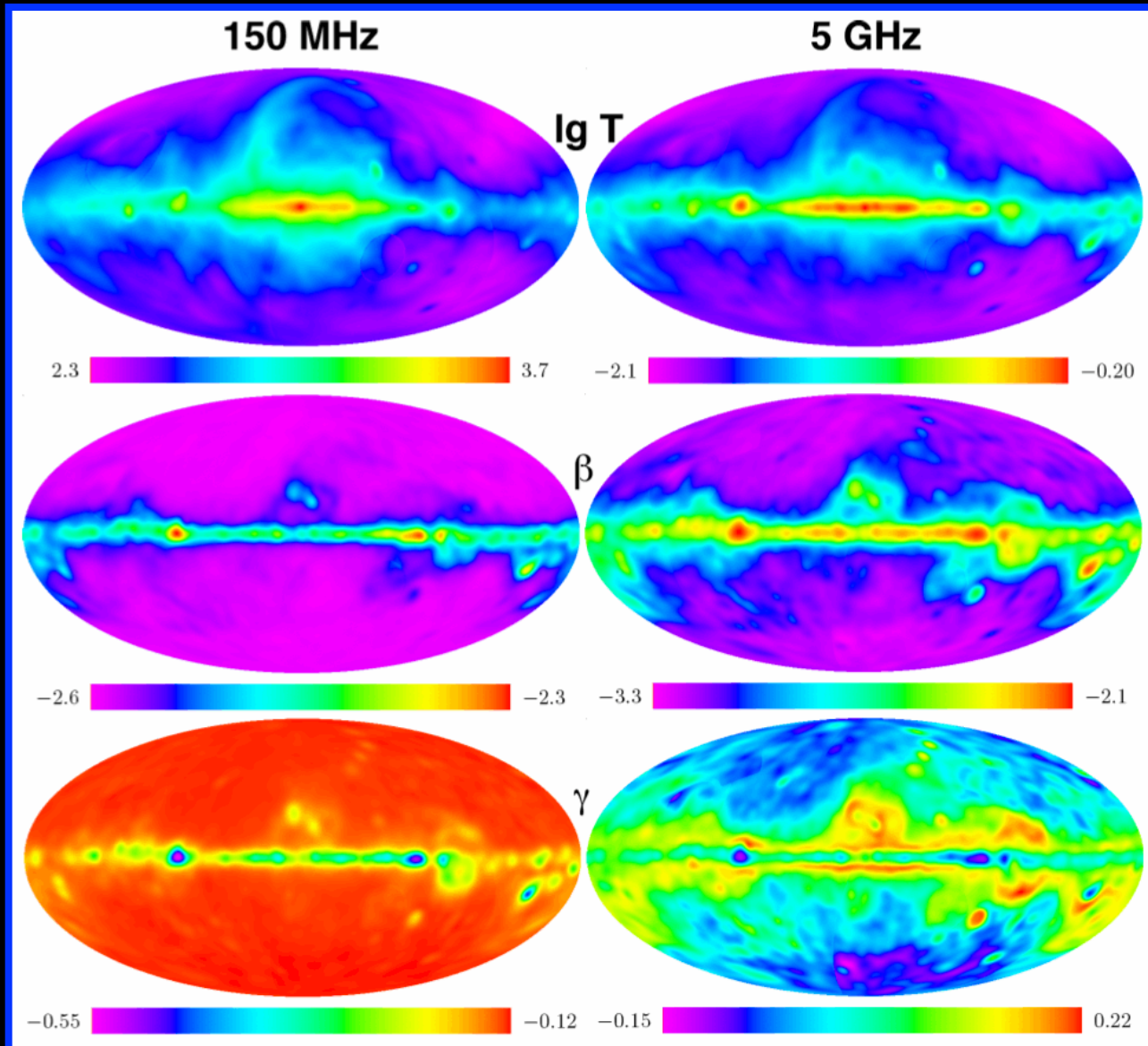


dust spinning dust



CMB Foreground Simulations

Modeling the diffuse emission from 10 MHz to 100 GHz



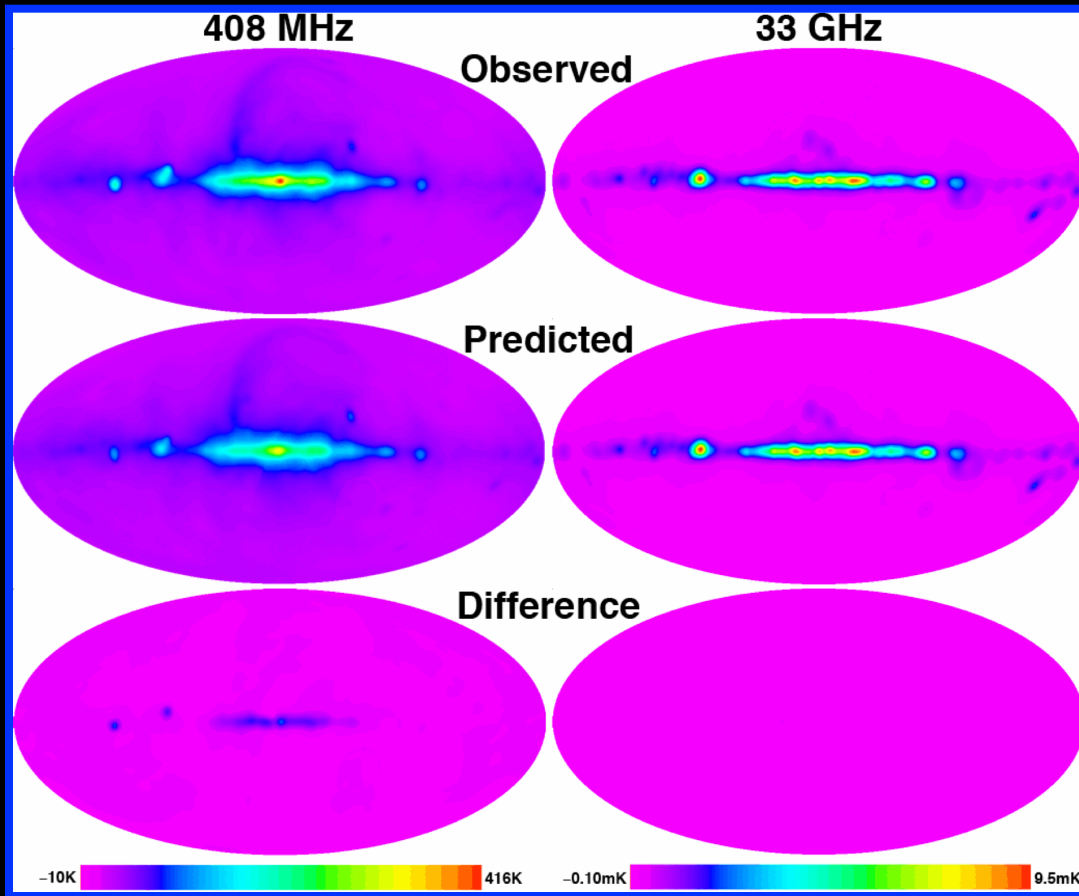
CMB Foreground Simulations

Modeling the diffuse emission from 10 MHz to 100 GHz

Comparison between data & model, how good is our fit?

The predicted map is constructed **without** using the data from that original frequency.

Relative rms error in the sky region 123456.

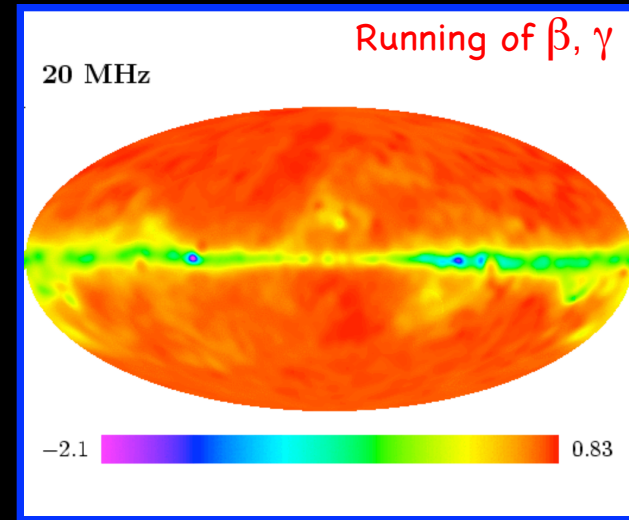
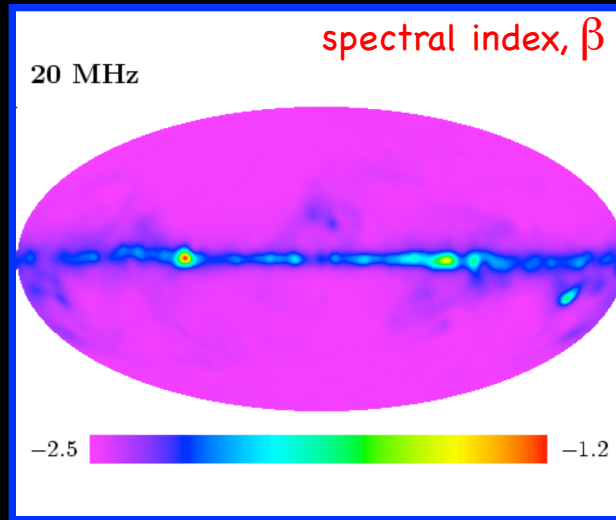
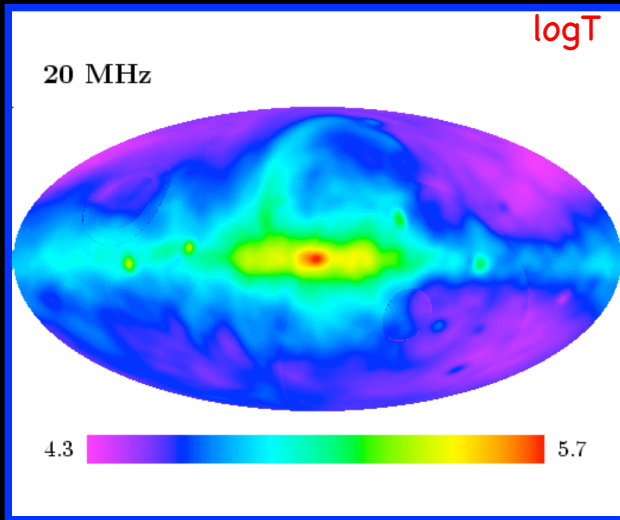


ν [GHz]	Optimal	Principal components used				
		1	2	3	4	5
0.010	0.062	0.543	0.078	0.072	0.065	0.066
0.022	0.036	0.450	0.064	0.060	0.039	0.038
0.045	0.035	0.438	0.046	0.046	0.038	0.038
0.408	0.034	0.379	0.044	0.044	0.039	0.039
1.420	0.111	0.386	0.135	0.135	0.150	0.196
2.326	0.075	0.235	0.084	0.083	0.081	0.137
23	0.015	0.463	0.058	0.026	0.026	0.026
33	0.006	0.504	0.086	0.009	0.008	0.008
41	0.009	0.519	0.089	0.017	0.015	0.015
61	0.018	0.542	0.023	0.023	0.023	0.023
94	0.057	0.538	0.225	0.059	0.059	0.059

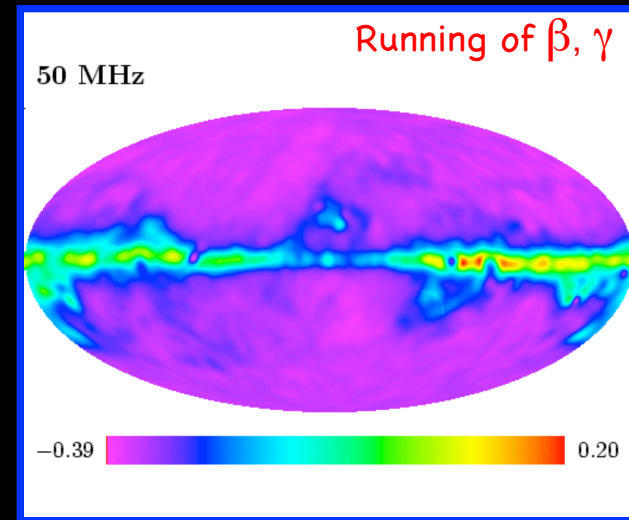
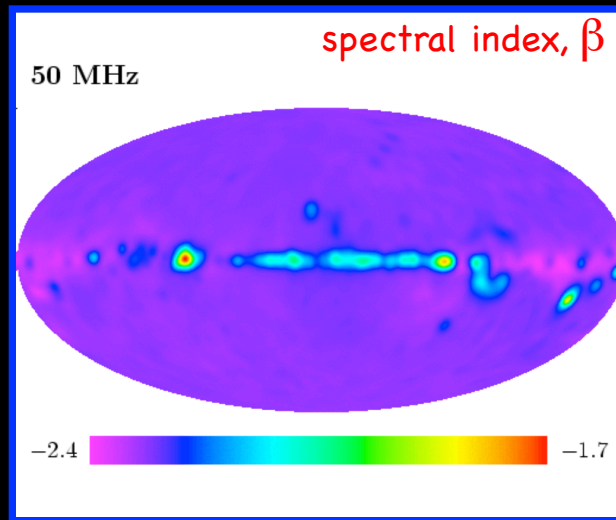
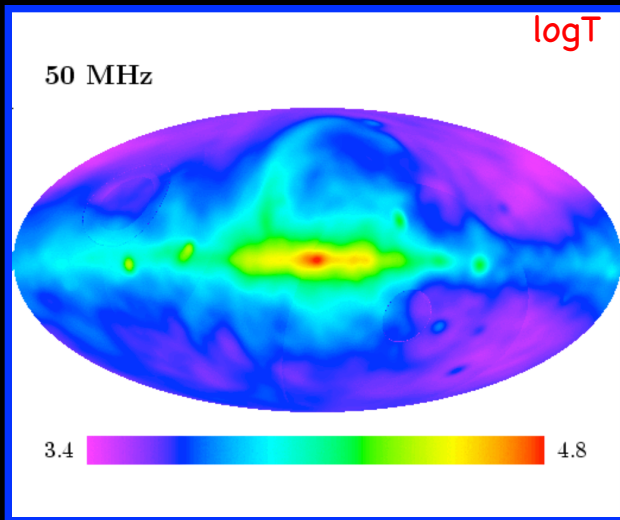
CMB Foreground Simulations

Modeling the diffuse emission from 10 MHz to 100 GHz

Movies:



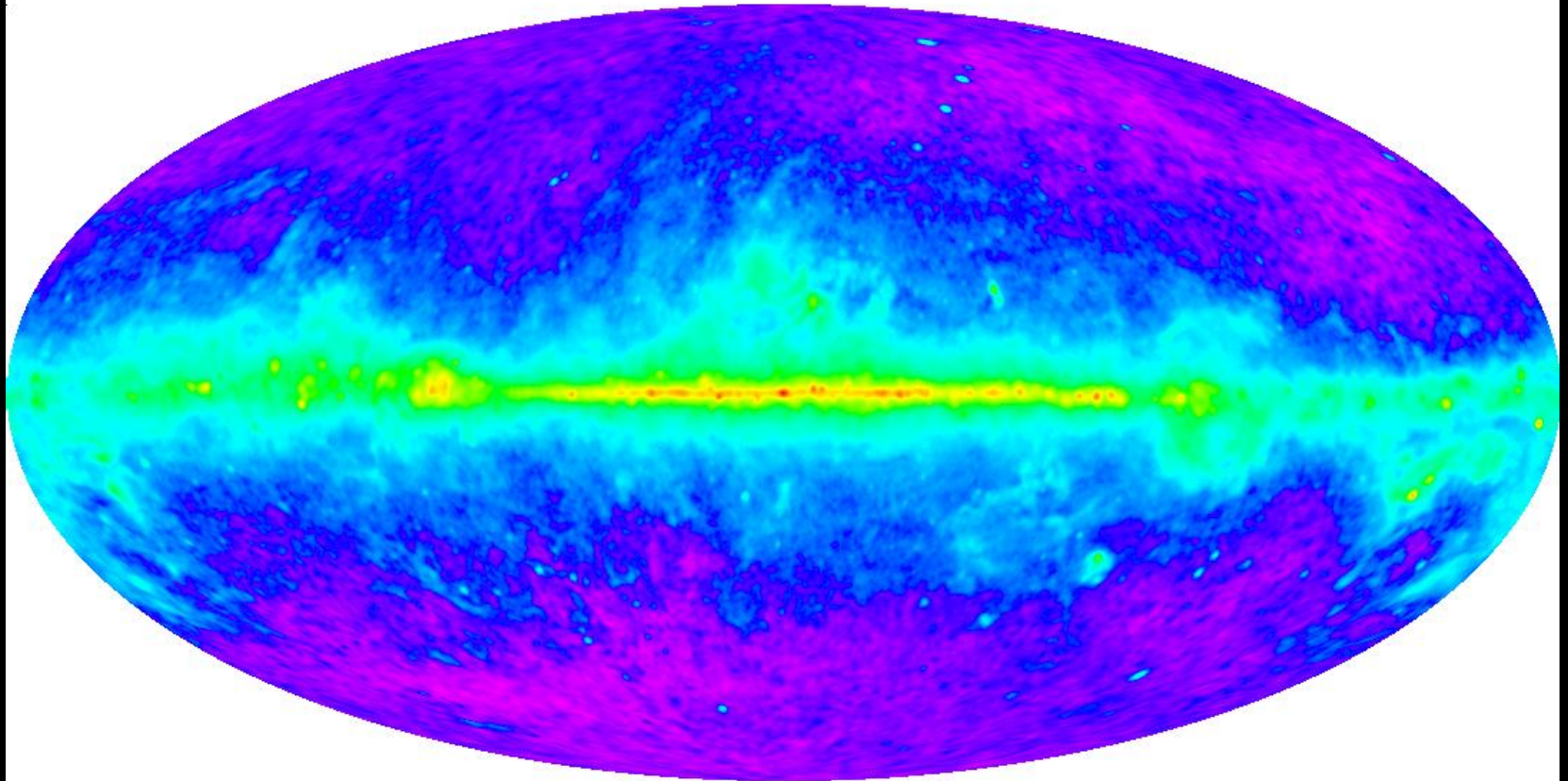
Movies, MWA range :



CMB Foreground Simulations

Modeling the diffuse emission from 100 GHz to 3000 GHz

100 GHz



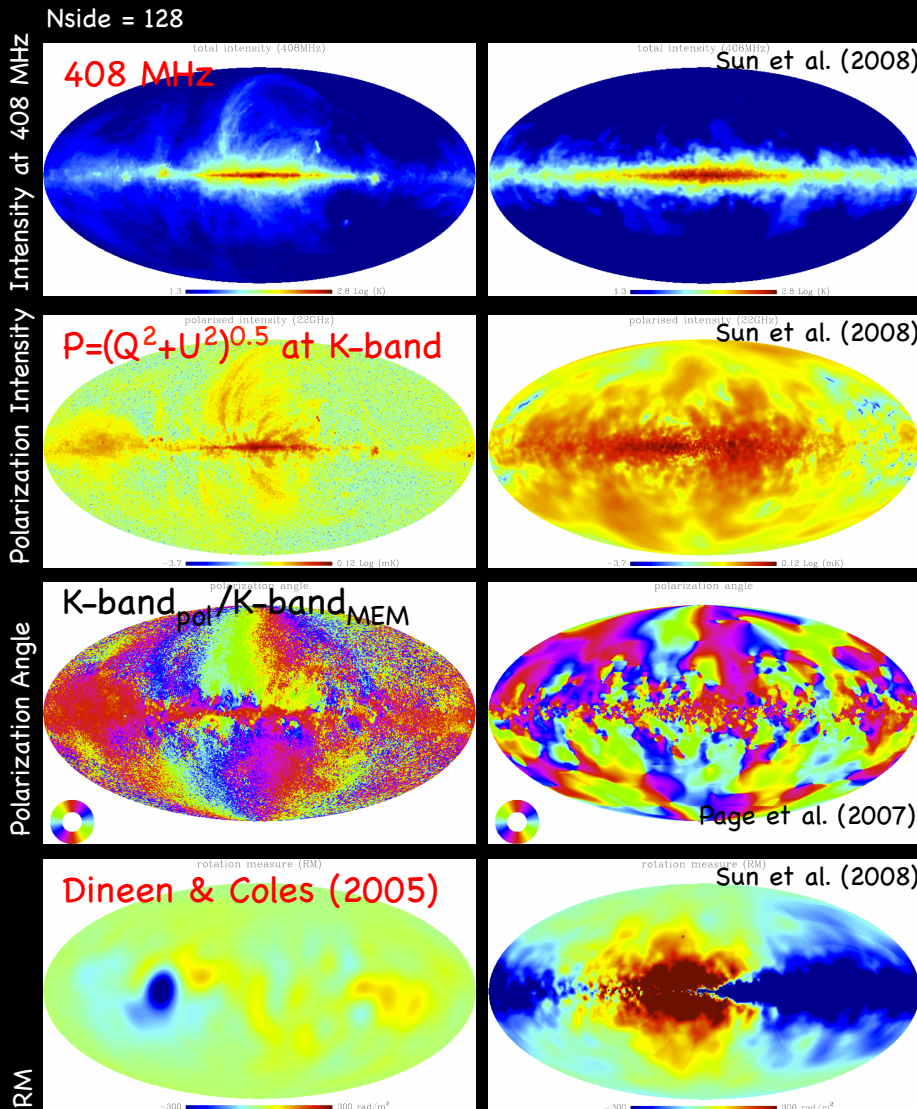
-0.43



3.4

CMB Foreground Simulations

Polarized Synchrotron Emission: Presented yesterday by Wolfgang



The **HAMMURABI** code (Waelkens et al. 2009) is a tool for simulating RM maps, total and polarized Galactic synchrotron emission maps. The input parameters of the code are the Galactic magnetic field B , the thermal electron density n_e and the cosmic-ray electron distribution ρ . n_e is model from NE2001 (Cordes and Lazio 2002), while assumptions are made about B and ρ .

This code can be downloaded from:

<http://www.mpa-garching.mpg.de/hammurabi/index.html>

CMB Foreground Simulations

Polarized Synchrotron + Dust Emissions: Presented yesterday by Lauranne

Fauvet et al. (2010) present a model of the polarized Galactic synchrotron and dust emissions. They produce a 3D model of the Galactic magnetic B-field which includes regular and turbulent components, and the distribution of matter in the Galaxy, the thermal electron density n_e and dust grains. The integration along the line-of-sight is done using the **HAMMURABI** code.

3D Galactic Magnetic Field: Presented yesterday by Wolfgang

From a comparison of simulated and observed maps, Sun et al. (2008) constrain the regular large-scale Galactic magnetic field in the disk and in the halo of the Galaxy. They find a 3D Galactic model that fits the observed Galactic total intensity and polarized emission better than other models over a wide range of frequencies. In addition, their model also agrees with the observed RMs from extragalactic sources.

CMB Foreground Simulations

Point Sources, Clustering of Sources

At the CMB frequencies ($1.4 \text{ GHz} < \nu < 150 \text{ GHz}$), the clustering of sources is known to be weak (Toffolatti et al. 1998, 1999; Blake & Wall 2002); while at the FIR frequencies, the clustering signal becomes relevant (eg, Gonzalez-Nuevo et al. 2005).

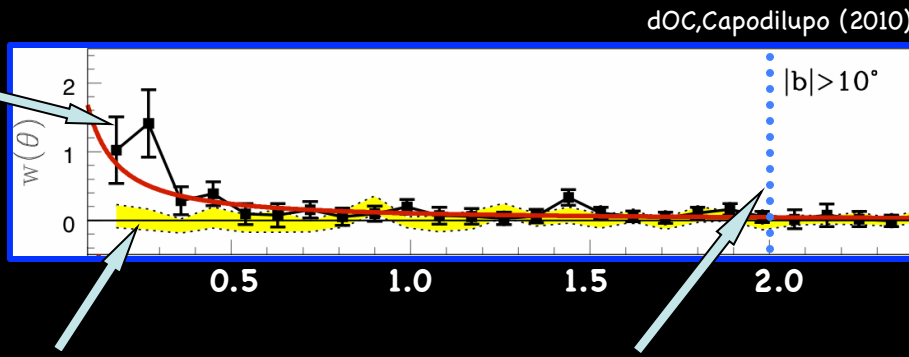
The distribution of radio sources is found to obey Poisson statistics with an observed angular clustering (see, e.g., Black et al. 2004; Cress et al. 1996). The clustering of astronomical sources is quantified using the angular 2-point correlation function, $w(\theta)$, with shape (Hamilton 1993):

$$w(\theta) = [DD(\theta) * RR(\theta)] / DR^2(\theta) - 1$$

A single power-law with shape $w(\theta) = A \theta^{-\gamma}$ fits the data well.

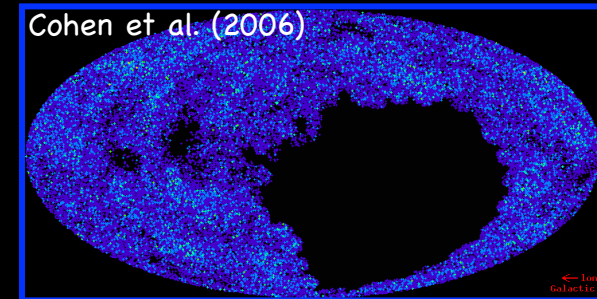
The amplitude of clustering has length of $0.2^\circ - 0.6^\circ$, and it is independent of the flux-density threshold.

The fall-off or break in $w(\theta)$ is due to the failure of the survey to resolve weak double sources with separations slightly greater than the beamwidth.



The mock correlations, as expected in a Poissonian distribution, have $w(\theta)$ consistent with zero.

$w(\theta)$ is consistent with zero. This is a strong evidence of uniformity in the survey.



0.1Jy/beam noise, 358 $14^\circ \times 14^\circ$ images, $S_c = 770 \text{ mJy}$, FWHM = $1.3'$, $N = 68,311$

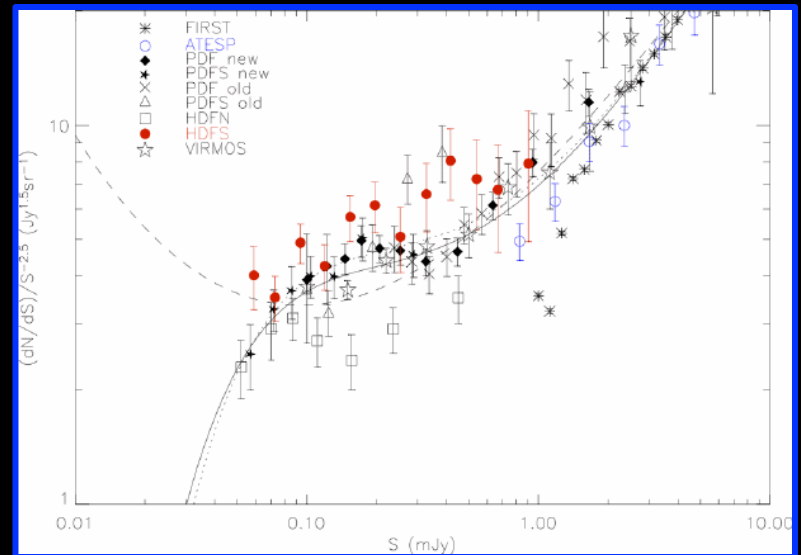
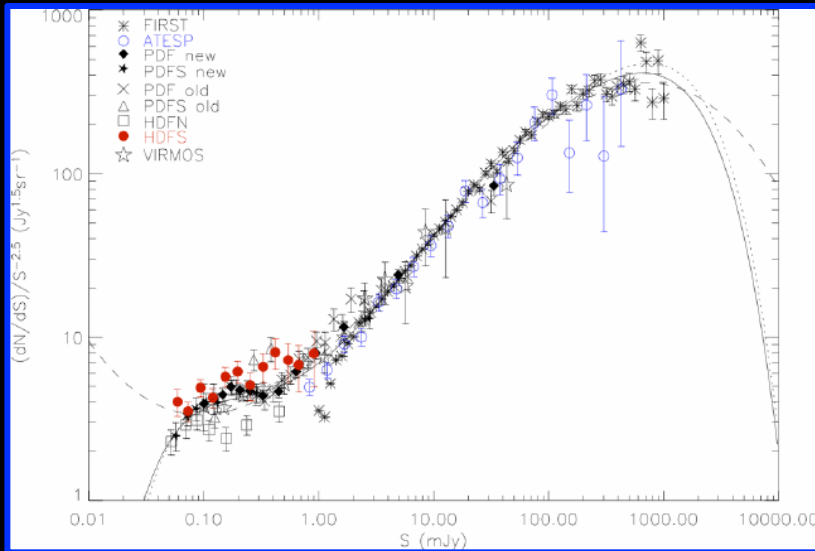
CMB Foreground Simulations

Point Sources, Source Counts

We adopted the source counts given by Huynh et al. (2005). The solid line is a sixth order polynomial fit to this compilation of source counts:

$$\text{Log} [(dN/dS)/S^{-2.5}] = \sum_{i=0,6} a_i [\text{log}(S/\text{mJy})]^i,$$

$$\text{with } a = (0.841, 0.540, 0.364, -0.063, -0.107, 0.052, -0.007)$$



CMB Foreground Simulations

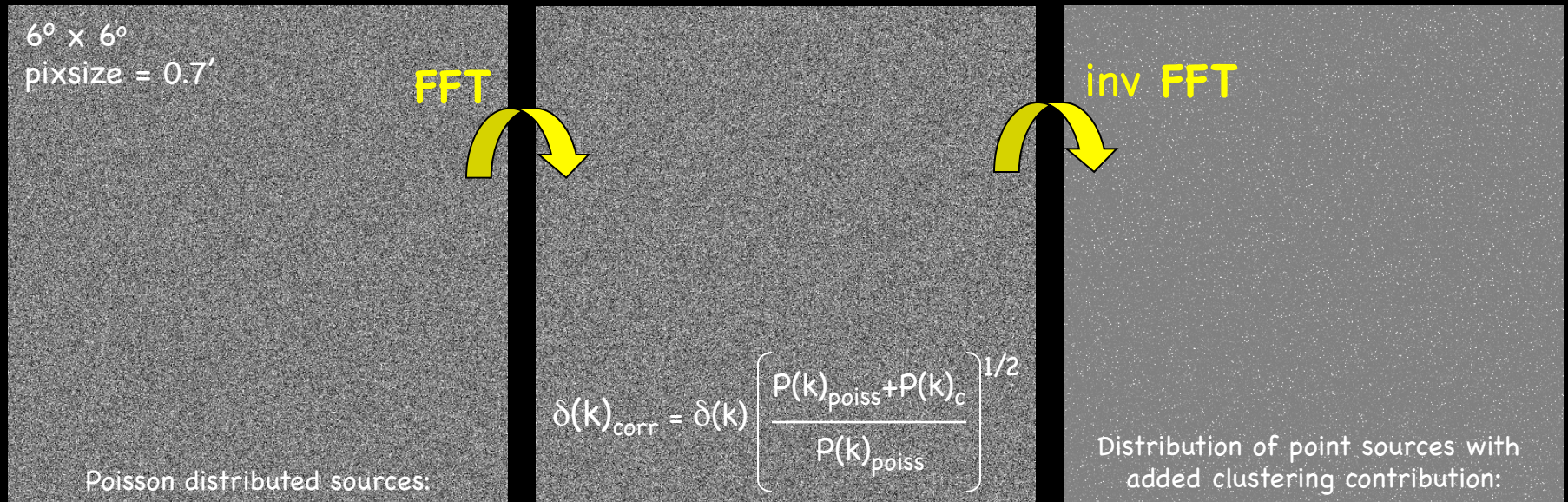
Argueso et al. (2003), Gonzalez-Nuevo et al. (2005)

First, we populate a $6^\circ \times 6^\circ$ map by adopting a simple Poisson distribution for the number of sources per pixel $n(x)$, where the mean of $n(x)$ is the average number of sources per pixel ($\langle n(x) \rangle = N(>S_{\min})/N_{\text{pix}}$). We define a projected density contrast $\delta(x) = [n(x) - \langle n \rangle] / \langle n \rangle$, where the covariance function of $\delta(x)$ is the usual 2-point correlation function $w(\theta) = \langle \delta(x) \delta(x+\theta) \rangle$.

The basic idea is to obtain a density field from a given power spectrum $P(k)$ or, equivalently, a given angular correlation function $w(\theta)$. We do this by calculating the FT of the density contrast $\delta(x)$, and obtaining its power spectrum $P(k)_{\text{poiss}}$.

$w(\theta)$ is added as a density contrast in Fourier space:

Then, we apply the inverse FT to $\delta(k)_{\text{corr}}$ to recover the new density field $\delta(x)_{\text{new}}$ and the modified number of point sources in each position of the map $n(x)_{\text{new}} = [1 + \delta(x)_{\text{new}}] \langle n \rangle$.



CMB Foreground Simulations

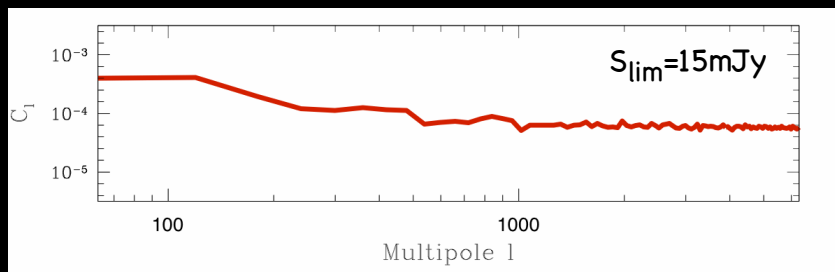
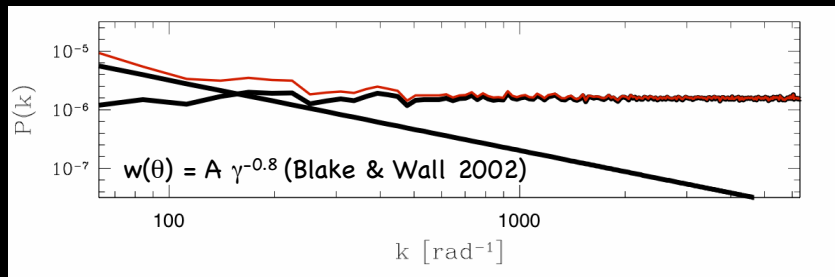
Argueso et al. (2003), Gonzalez-Nuevo et al. (2005)

We now can convert the counts $n(x)$ into fluxes...

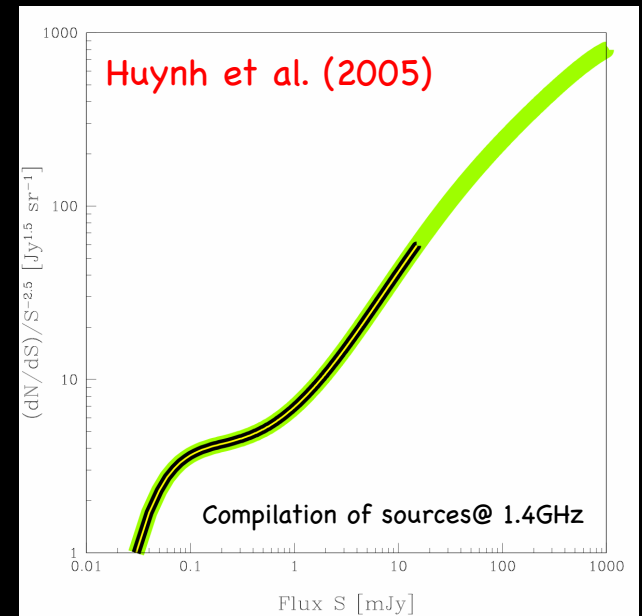
“Life is like a sewer... what you get out of it depends on what you put in...” (Tom Lehrer)

We need to know the differential counts dN/dS at a given frequency ν (and, in principle, for each source population). This gives us the number of sources $N(S)$ at each flux interval, and

we need to have an efficient algorithm for distributing the fluxes in a map – ie, our simulations should recover dN/dS and the “input” $w(\theta)$ has to be reconstructed at least down to the flux limit of the sample by which $P(k)$ has been determined.



dOC, Bernardi, Gonzalez-Nuevo, +, in prep.



At first approach, we distribute the fluxes at **random** among the pixels; and simulations are read in a few seconds.

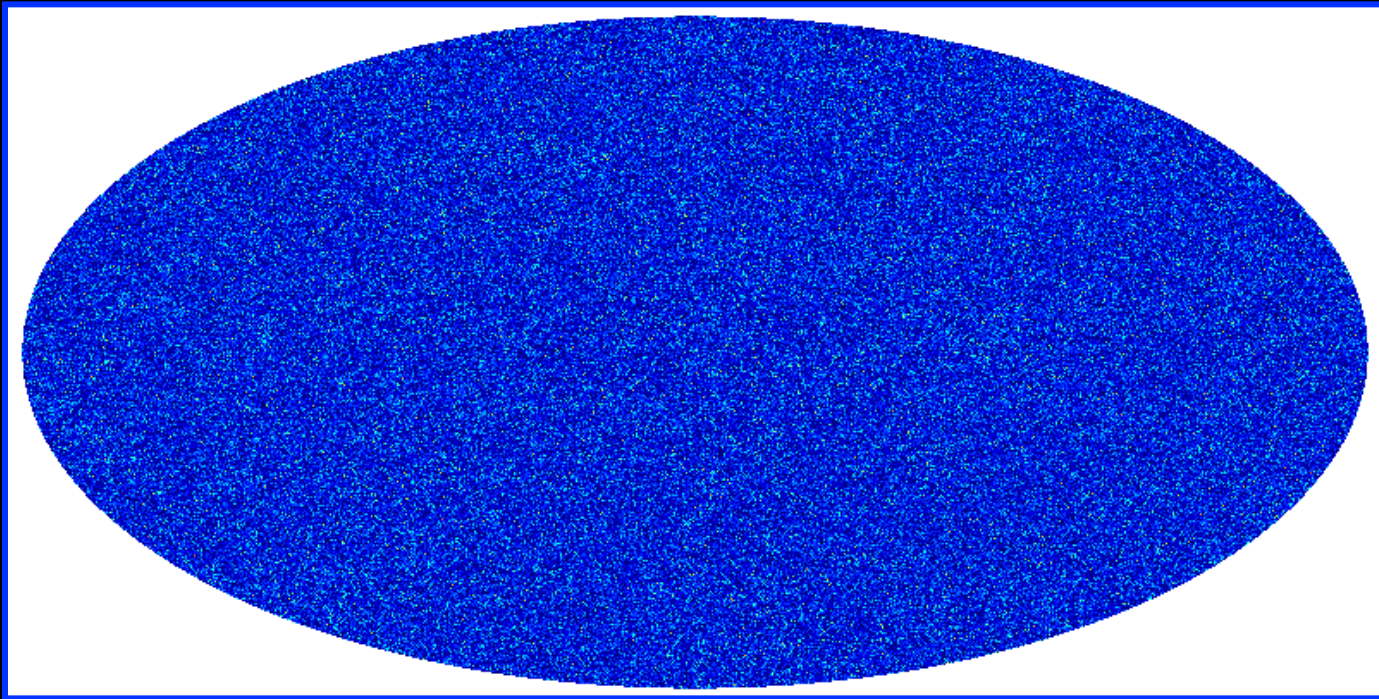
CMB Foreground Simulations

Argueso et al. (2003), Gonzalez-Nuevo et al. (2005)

We produce all sky-maps by calculating

$$\delta T/T = a_{lm} Y_{lm},$$

where the a_{lm} are estimated using the subroutine anafast from HEALPix package (Gorski et al. 2002).

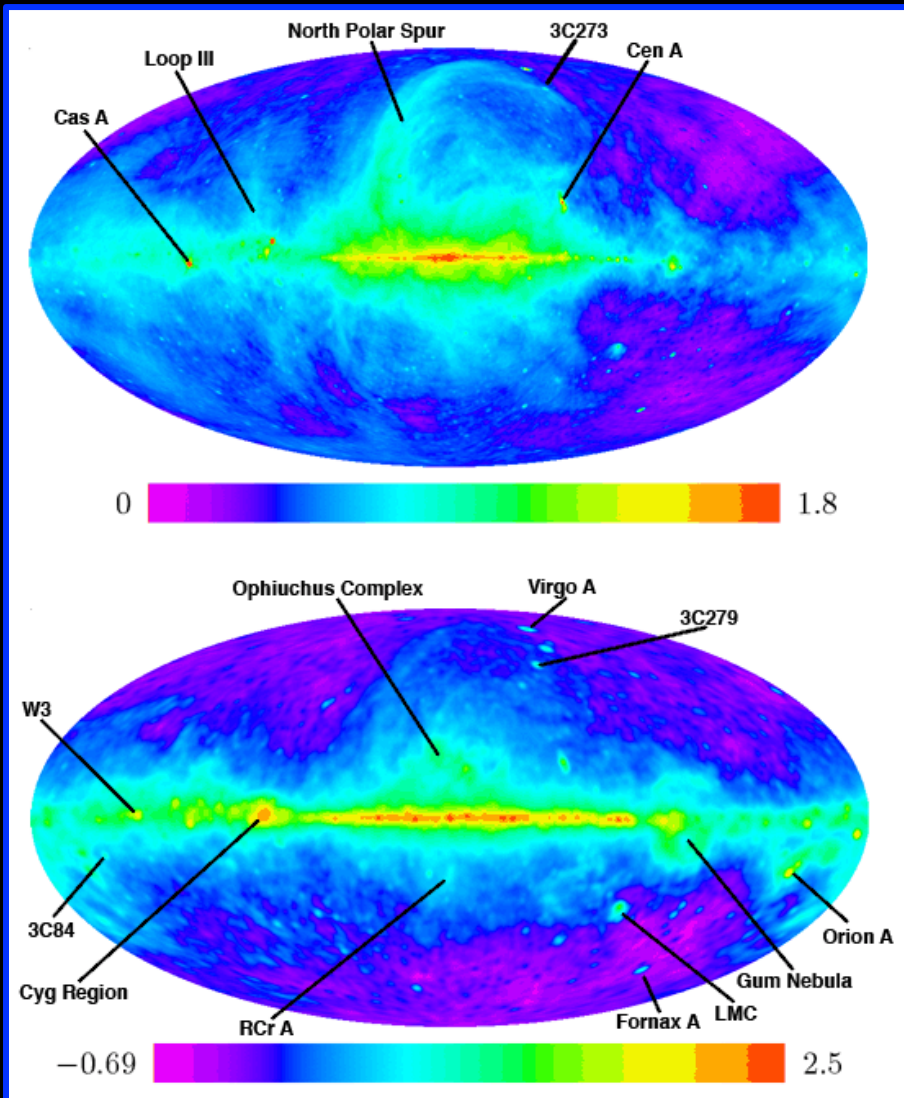


$N_{\text{side}} = 512$

Also implemented in the PSM.

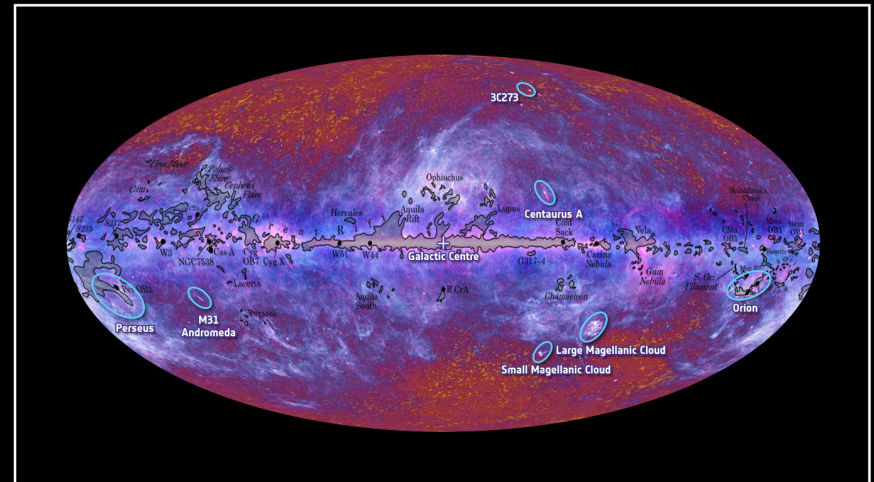
CMB Foreground Simulations

Conclusions / Discussions



Why people do foreground simulations?

Simulations are a vital: accurate modeling and subtraction of the foreground contamination is necessary in order to correct the measured CMB power spectrum. To do a good job on removing foregrounds, we need to understand their frequency and scale dependence, frequency coherence, and better characterize their non-Gaussian behavior. In addition, foreground simulations also help to optimize scan strategy and data analysis pipelines.



<https://www.cfa.harvard.edu/~adeolive/gsm/> or
<http://lambda.gsfc.nasa.gov/toolbox/>